Spray Coating Experiments: Setups and Methodologies

The latest eBook from Advanced Optical Metrology. Download for free.

Spray Coating Experiments: Setups and Methodologies, is the third in our Thin Films eBook series. This publication provides an introduction to spray coating, three article digests from Wiley Online Library and the latest news about Evident's Image of the Year Award 2022.

Wiley in collaboration with Evident, are committed to bridging the gap between fundamental research and industrial applications in the field of optical metrology. We strive to do this by collecting and organizing existing information, making it more accessible and useful for researchers and practitioners alike.

EVIDENT
OLYMPUS

WILEY

Self-Assembly of Hydrophilic Homopolymers: A Matter of RAFT End Groups

*Jianzhong Du, Helen Willcock, Joseph P. Patterson, Ian Portman, and Rachel K. O'Reilly**

*Unusual self-assembly behavior is observed for a range of hydrophilic homopolymers. This self-assembly behavior is contrary to the expected behavior of such hydrophilic polymers and instead mimics more commonly reported amphiphilic block copolymers. It is proposed that the unique combination of hydrophobic end groups at both the α and ω chain end accounts for this unusual self-assembly behavior. Complex internal polymer micelles are spontaneously formed when hydrophilic homopolymer polyelectrolytes and neutral polymers (with a weight fraction of the hydrophobic end groups <10 wt%) are directly dissolved in water. The homopolymers, poly[2-(diethylamino)ethyl methacrylate], poly(*N*-isopropylacrylamide), and poly(ethoxyethylacrylate) are synthesized by reversible addition–fragmentation chain-transfer (RAFT) polymerization using S′-1-dodecyl-(S′)-(α,α′-dimethyl-α′′-acetic acid) trithiocarbonate (DDMAT) and its derivatives as chain transfer agents (CTAs). A range of polyelectrolyte homopolymers with different terminal groups are designed and synthesized, which under acidic aqueous solution direct the self-assembly to form well-defined nanostructures. This assembly behavior was also observed for neutral polymers, and it was determined that the structure of the hydrophobic end groups (and thus choice of RAFT CTA) are very important in facilitating this unusual self-assembly behavior of hydrophilic homopolymers. It is proposed that the functionality of commonly used CTAs such as DDMAT, can affect the solution association of the resultant homopolymers and can in fact afford ABA′ type polymers, which can undergo self-assembly to form higher-order nanostructures.*

1. Introduction

It has been well documented in recent decades that the self-assembly of amphiphilic block copolymers can form a range of different nanostructures such as spherical micelles, vesicles, and cylinders.[1–6] Even though self-assembly is influenced by a number of factors,[7,8] a suitable hydrophilic–hydrophobic balance in the amphiphilic polymer is required to form higher-order structures, and the morphology afforded depends on this ratio that is classically described as the dimensionless 'packing parameter', *p*.[9] Overall the factors that control the morphology of the resultant nanostructure include the chemical structure of the copolymer, the hydrophobic/hydrophilic ratio, copolymer concentration in solution, and the solvent properties.[10] The hydrophobic/hydrophilic ratio in the polymer is proposed to be perhaps the important parameter in the self-assembly process.[11] As a general rule, copolymers with <50 vol.% hydrophobic block usually form micelles; copolymers with ~50–66 vol.% hydrophobic block usually favor vesicle formation; those with

Dr. J. Du, Dr. H. Willcock, J. P. Patterson, Dr. R. K. O'Reilly
Department of Chemistry
Gibbet Hill Road, University of Warwick, CV4 7AL, UK
E-mail: r.k.o-reilly@warwick.ac.uk
I. Portman
Electron Microscopy Facility
Department of Life Sciences
University of Warwick, CV4 7AL, UK

DOI: 10.1002/smll.201100382

small NANO MICRO

more than 66 vol.% of hydrophobic proportion may form vesicles, inverted microstructures, other complex structures such as compound micelles, and finally macroscopic precipitates. That is to say, polymers with a low hydrophobic content favor spherical micelle structures in polar solvents where the hydrophobic portion forms a core excluding solvent molecules and the hydrophilic corona is expressed from the core to stabilize the colloidal structure. An increase in the relative hydrophobicity usually leads to the formation of nanostructure morphologies such as polymer vesicles or at extremely high hydrophobic contents compound micelles.[12] Indeed, the self-assembly of amphiphilic diblock copolymers is a very well-established and exploited field compared to the area of homopolymer self-assembly.

In recent years there has been increasing interest in the application of homopolymers for the formation of nanostructures using conventional self-assembly approaches, given their relative ease of synthesis compared to diblock analogues. For example, Cha et al. reported that positively charged poly(L-lysine) polyelectrolytes could interact with negatively charged semiconductor nanocrystals to co-operatively self-assemble into vesicles in water with quantum dots in the membrane.[13] It should be noted that in these cases, the poly(L-lysine) homopolymer in the absence of the quantum dots does not form nanostructures in water. In addition, Thayumanavan et al. have reported a range of supramolecular assemblies from amphiphilic homopolymers.[14,15] For example, an amphiphilic polyacrylamide homopolymer (number-averaged molecular weight, $M_n \approx 10$ kDa) whose repeating unit consisted of a grafted relatively long hydrophobic chain (8 carbon atoms) and a short hydrophilic head group (one carboxylic acid group) can form hollow structures in water whereas homopolymers with a shorter or longer hydrophobic chain in the repeating unit form spherical micelles.[16] Additionally, hydrophically modified comblike polybutadienes with a hydrophilic fraction of 0.11–0.55 have also been explored for the synthesis of vesicle-type structures.[17] More recently, work by Cheng and co-workers utilized giant silsesquioxane-polystyrene surfactants in self-assembly to form a range of nanostructured morphologies.[18] All of these previous examples of homopolymer self-assembly have a hydrophobicity fraction that predicts vesicle formation, regardless of whether the hydrophobicity originates from the polymer backbone or side chains. However in recent years there has been increasing interest in using competing mechanisms for the self assembly of well-defined aggregates such as discs, cylinders, and vesicles. These include the exploration of using crystallization-driven self assembly,[19,20] electrostatic interactions,[21,22] architecturally complex polymers,[23] or midblock interactions[24] for the well-defined assembly of polymers into morphologies not predicted based on packing parameter considerations. In this work, we were interested in exploring the effect of end groups on the self-assembly of hydrophilic homopolymers. It is well-known that the introduction of hydrophobic end groups in thermally responsive polymers such as *N*-isopropylacrylamide (NIPAM) has an effect on the lower critical solution temperature (LCST) behavior,[25] and the effect of hydrophobic end groups on the self assembly of hydrophilic homopolymers is also well-established.[26,27] Indeed in the 1990s seminal theoretical papers by Rubinstein and Semonov described the self assembly of such associating and telechelic polymers.[28–31] These studies have mainly focused on utilizing polyethylene glycol or poly(*N*-isopropylacrylamide) (PNIPAM) with alkyl end groups, with these materials finding application as rheology modifiers and coatings.[32–35]

Given the recent advances in controlled radical polymerization (CRP) techniques, the ability to tune and tailor the polymer end group has now been fully realized. This is especially true for polymers prepared by reversible addition-fragmentation chain transfer polymerization (RAFT),[36–38] in which both α and ω chain end functionality can be incorporated into the chain transfer agent, or introduced postpolymerization using established end group modification methods.[39–41] The effect of the RAFT end group on the self-assembly has seldom been considered in the past due to the very small weight fraction compared to the polymer chain; however in this work we propose that the end groups can indeed play a significant role in directing self-assembly.

There have been few reports on the selective introduction of hydrophobic end groups into hydrophilic homopolymers prepared by RAFT methods. In 2005, Winnik and co-workers explored the self-assembly of PNIPAM prepared by RAFT and terminated at both ends by long alkyl chains (C18) to form an ABA type triblock.[42] Further work from this group in collaboration with Koga in 2008, reported the construction of a theoretical model to account for the concentration and temperature-dependent properties of such polymers.[43] In this work they reported that the polymers formed flowerlike micelles in the dilute regime and a network of micelles when concentrated. Indeed, a very recent paper by Davies, Lowe, and co-workers, highlights that through the selective introduction of two close rigid rings at the ω-terminus of hydrophilic homopolymers, well-defined vesicles can be formed.[44] In this work the authors proposed that the presence of the two spatially close rigid rings at the ω-terminus was key in the formation of well-defined aggregates. In contrast to these previous reports, we were interested in examining the effect of a commonly utilized chain transfer agent, *S*′-1-dodecyl-(*S*′)-(α,α′-dimethyl-α′′-acetic acid) trithiocarbonate (DDMAT) and its simple derivatives, on the self-assembly of hydrophilic homopolymers, rather than the selective introduction of hydrophobicity into the RAFT agent. We were particularly interested in DDMAT as it contains a hydrophobic dodecyl chain as part of the Z group and has a carboxylic functionality (as part of the R group), which at low pH will be less polar and hence less hydrophilic. We thus proposed at low pH hydrophilic polymers prepared using this RAFT agent would have an ABA′ type structure, which has been shown previously to self-assemble into a range of nanostructure morphologies.[45,46]

Hence, in this work we report well-defined nanostructure formation from the self-assembly of a hydrophilic and charged homopolymers in acidic water with hydrophobic fractions (which originate from both α and ω hydrophobic end group functionality) as low as 2 wt%. Our findings lead us to propose that nanostructure formation from hydrophilic and charged homopolymers does not obey the traditional

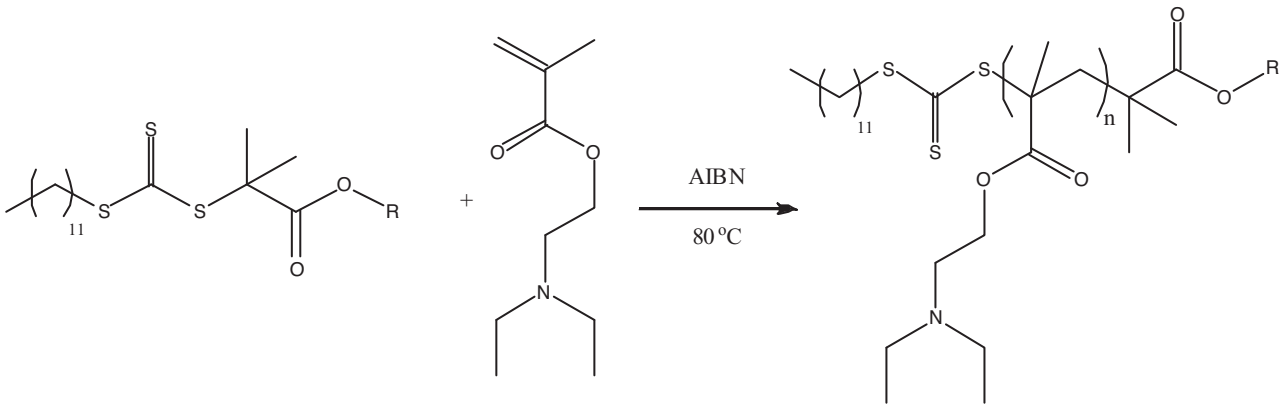

Scheme 1. Polymerization of DEA using a range of trithiocarbonate chain transfer agents (CTAs). AIBN represents (2,2′-azobis(2-methylpropionitrile)).

rules of polymer self-assembly, and instead a focus on the subtle effects of polymer end groups should be considered rather than just considerations of the hydrophilic weight fraction. Furthermore the observations of well-defined self-assembly were also confirmed for neutral polymers at low pH and using modified DDMAT derivatives. These results are important as the effect of RAFT end groups on the self-assembly is often ignored given their low weight fraction; however we propose that more careful consideration should be given to their influence on self-assembly processes. Finally, we propose that such RAFT-prepared hydrophilic homopolymers may present more synthetically accessible alternatives for applications in self-assembly, compared to conventional amphiphilic diblock copolymers.

2. Results and Discussion

2.1. Design and Synthesis of Hydrophilic Homopolymers

Following on from some initial work in the area of diblock copolymer self-assembly we found that the nature of the hydrophobic end groups in these polymers influenced the resultant self-assembly behavior.[47] The self-assembly of homopolymers is of great interest given the easier synthesis; however controlling the morphologies of the resultant nanostructures has not been explored in depth. To explore this we utilized α and ω end group functionalized hydrophilic polymers to explore their effect on the self-assembly process. Our initial investigations explored a range of polyelectrolyte (poly(*N*,*N*-diethylacrylamide), PDEA) homopolymers with different end groups, which were designed and synthesized by RAFT, as shown in **Scheme 1**. All these homopolymers were protonated by HCl aqueous solution during the purification process to afford homopolymer polyelectrolytes. Previous work in our group has demonstrated that the trithiocarbonate end group is stable for many months under these conditions.[47]

Polymers **1**–**3** in **Figure 1** were synthesized by the RAFT polymerization of DEA with carefully chosen α and ω terminal hydrophobic groups introduced by the choice of chain transfer agent, which were all based around the commonly used DDMAT structure. Specifically, the effect of the long dodecyl chain, which is often employed as a Z group in trithiocarbonates was explored, as was the effect of different hydrophobic R groups. Polymers **4** and **5** were synthesized by atom transfer radical polymerization (ATRP) with only one terminal hydrophobic end group. Polymer **1** has a hydrophobic, fluorescent pyrene group (Py) at the α position and a hydrophobic dodecyl (D) group at the ω position. In polymer **2** the pyrene group was replaced by $-C(CH_3)_2COOH$ (C), which was hydrophilic above neutral pH and less polar at low pH. In polymer **3** the C group was replaced by an ethyl ester functionality $-C(CH_3)_2COO-CH_2CH_3$ (E), which is permanently hydrophobic and not pH sensitive. Polymers **4** and **5** only have a single hydrophobic group either Py or E respectively, as their chain end and were used as control systems. Table S1 in the Supporting Information (SI) reports the molecular weights and molecular weight distributions of the deprotonated PDEA homopolymers (**1**–**5**). A noncharged polymer, PNIPAM, was also synthesized with a Py and a D group (**6**) or with a C and D group (**7**) as well as poly(ethoxyethylacrylate) (PEEA) with a Py and D group (**8**) as additional controls. Given the difficulty in determining the molecular weight by gel permeation chromatography (GPC) analysis (due to the highly polar nature of the polymers and lack of relevant standards), the molecular weight of the polymers were calculated by comparing the integrated areas of pyrene end groups (peak j) and PDEA side chains such as peaks b and c in a good solvent for all segments of the polymer chain (see **Figure 2**). The molecular weight and molecular-weight distribution, as well as the weight fraction of the end group in the whole polymer are summarized in the Table S1 (SI). The weight percentage of the end groups in the homopolymer are all very low, ranging between 1% and 4% except for polymer **1.1** which has a higher weight percentage of 10.2%.

2.2. Self-Assembly of Homopolymers

The self-assembly of the PDEA homopolymers were easily performed by dissolving the homopolymer in acidic water at pH 2 at ~5 mg/mL. The self assembly of the polymers **1**–**5** was initially studied by analysis using ^{1}H NMR spectroscopy. In

small NANO MICRO

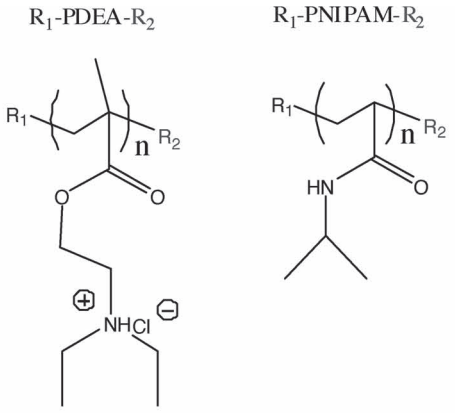

	Polymer	R_1	R_2	n
1.1	Py-PDEA-D	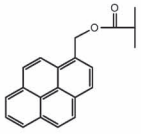	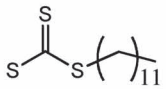	23
1.2				76
1.3				122
1.4				150
2	C-PDEA-D	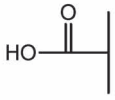	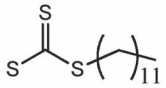	76
3	E-PDEA-D	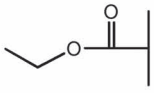	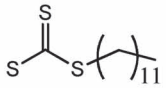	74
4	Py-PDEA-Br	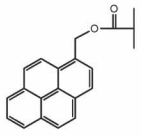	Br	100
5	E-PDEA-Br	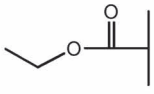	Br	82
6	Py-PNIPAM-D	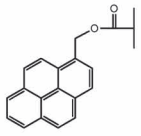	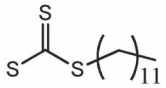	72
7	C-PNIPAM-D	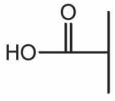	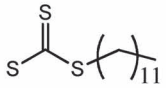	115
8	Py-PEEA-D	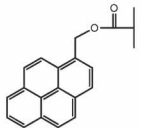	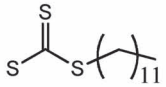	78

Figure 1. Homopolymers PDEA (**1**–**5**), PNIPAM (**6** and **7**), and PEEA (**8**) with different end groups.

the case of homopolymers with hydrophobic end groups at both the α and ω positions (**1**–**3**), a strong attenuation of their end groups upon dissolution in acidic water was observed. A typical ^{1}H NMR spectrum of Py-PDEA$_{76}$-D homopolymer (**1.2**) in D_2O at pH 3 is shown in Figure 2. The strong attenuation of Py and D groups suggests the hydrophobic terminal groups are aggregated together in the polar hydrophilic solution. In contrast, homopolymers (**4** and **5**) with only one hydrophobic end group do not behave in this manner and instead no significant attenuation of pyrene signal was found from the ^{1}H NMR spectrum of Py–PDEA$_{100}$–Br (**4**) in D_2O at pH 3 compared with the spectrum in its good solvent, $CDCl_3$/MeOD, as shown in Figure 2. The close proximity of the two hydrophobic end groups in aqueous solution was confirmed through identification of a cross peak in the 2D nuclear Overhauser enhancement spectroscopy (NOESY) NMR spectra (Figure S1, SI). This suggests that for the homopolymers with dual hydrophobic groups, self-assembly into higher-order structures may be occurring in water whereas the homopolymers with a single hydrophobic end group show no evidence of assembly under these conditions. Further evidence of this interaction of hydrophobic groups within a nonpolar environment was confirmed using fluorescence measurements, which indicated the pyrene groups were in a hydrophobic environment and also some quenching through excimer formation was observed.

The solution properties of the homopolymers in acidic water were compared and digital photos of the different homopolymer solutions are shown in **Figure 3**. Comparing the three nanostructure solutions made from Py–PDEA$_n$–D (**1.1**, **1.2**, and **1.4**) with the same pyrene and dodecyl end groups (n = 23, 76, and 150), the turbidity of the aggregate solution was observed to decrease with the increase of PDEA chain length, which suggests a decrease in particle size. Comparing the nanostructure solutions of Py–PDEA$_{76}$–D (**1.2**) and C–PDEA$_{76}$–D (**2**), the nanostructure solution with the pyrene end group is more turbid (and hence larger) than that with isobutyric acid groups, as a result of the higher hydrophobicity (rather than hydrophobic fraction) of pyrene compared to the isobutyric acid group. The solution of E–PDEA$_{74}$–D (**3**) (not shown) is slightly more turbid than that of **2**, but less turbid than **1.2** indicating that they are intermediate in size at the same concentration. This is consistent with the proposed order of decreasing polarity of the end group: acid < ethyl < pyrene, in which the most hydrophobic end

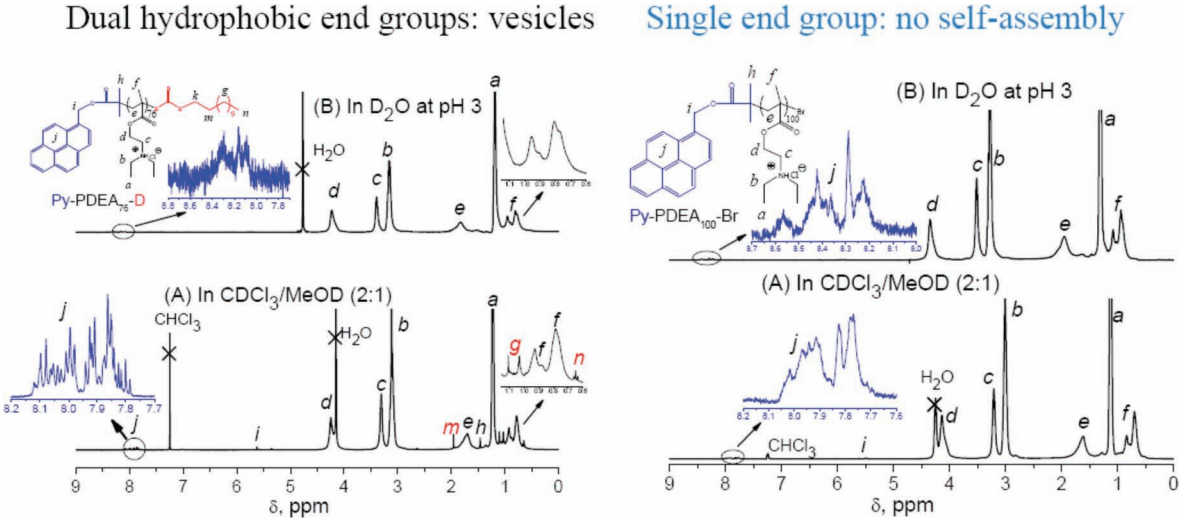

Figure 2. ^{1}H NMR spectra of homopolymers with dual hydrophobic end groups versus a single hydrophobic end group at 5 mg/mL. Left: Homopolymer **1.2**, Py-PDEA$_{76}$-D, with two hydrophobic end groups: A) in $CDCl_3$/MeOD (2:1), a good solvent for both polymer and end groups; B) in D_2O at pH 3, a nonsolvent for the end groups. The signals from pyrene (peak j, blue) and dodecyl (peaks g, n and m, red) in $CDCl_3$/MeOD are visible but remarkably attenuated in D_2O, indicating the aggregation of the pyrene and dodecyl groups in a polar hydrophobic environment. Right: Homopolymer **4**, Py-PDEA$_{100}$-Br, with one hydrophobic end group: A) in $CDCl_3$/MeOD (2:1); B) in D_2O at pH 3. The signals from pyrene (peak j, blue) in $CDCl_3$/MeOD are visible, and no obvious attenuation in D_2O was found, indicating loose or no aggregation of pyrene end group in a polar environment.

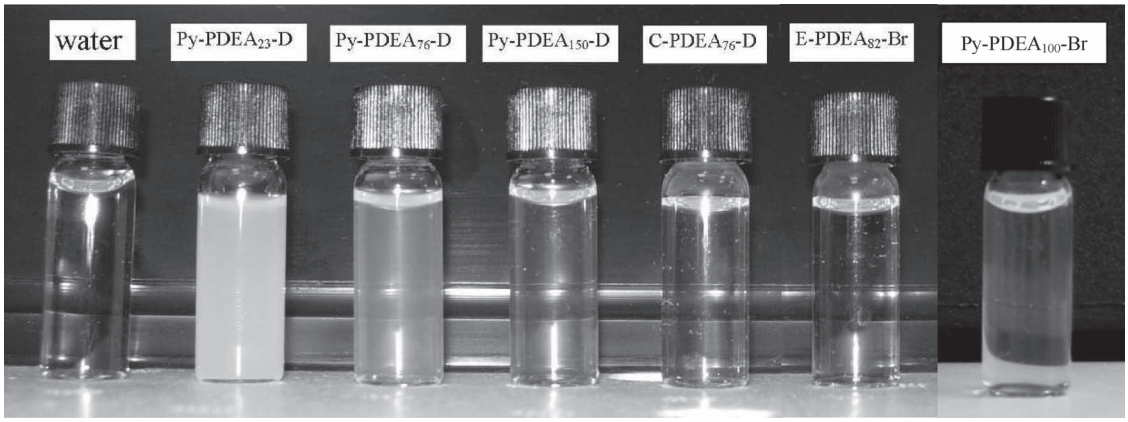

Figure 3. Digital camera image of nanostructure solution by direct dissolution of different homopolymers in water at pH 2 at 5.0 mg/mL.

group affords the largest particles. As a control, homopolymers **4** and **5**, which both only have a single hydrophobic end group were compared to the above results, and it is clear that these solutions are similar to that of pure water, indicating that no large aggregates were detected. This further indicates that dual hydrophobic end groups are required to effect the self-assembly of this charged hydrophilic homopolymer.

2.3. Dynamic Light Scattering (DLS) Studies of Self-Assemblies

DLS studies confirmed the above empirical observations and indicated the formation of regular structures upon the self-assembly of the homopolymers with two hydrophobic end groups (**1–3**) whereas no regular self-assemblies were found for homopolymers containing only one hydrophobic end group (**4** and **5**) (**Table 1**). As shown in Figure S2 (SI), the correlation functions revealed that when the concentration of polymer **1.2** was 0.1 mg/mL, the measured correlation function was too poor for Cumulant analysis, yet it improved upon increasing the polymer concentration. The correlation curve at 0.1 mg/mL decays to baseline within 500 μs, indicating the smaller and hence faster diffusing free polymer chains or ill-defined loose aggregates. However, the larger and slower diffusing particles prepared at higher polymer concentration (>1.0 mg/mL) required nearly 2000 μs before correlation in the signal is lost. The data quality from polymers **4** and **5** even at higher concentration (20 mg/mL) were still too poor to fit a Cumulant analysis, which further confirmed no self-assembly was observed for the homopolymers with only a single hydrophobic end group.

The correlation curve is a result of all the information regarding the diffusion of particles being measured. The diffusion coefficient (D) is calculated by fitting the correlation curve to an exponential function, with D being proportional to the lifetime of the exponential decay (Figure S2, SI). The hydrodynamic radius (R_h) is then calculated from the

small NANO MICRO

Table 1. DLS studies of nanostructures by direct dissolution of PDEA homopolymers at 5.0 mg/mL at pH 2 or PNIPAM homopolymer at pH 6 in water.

Code	Polymer[a)]	D_h [nm][b)]	D_h [nm][c)]	PD[d)]
1.1	Py–$PDEA_{23}$–D	255	226	0.207
1.2	Py–$PDEA_{76}$–D	150	142	0.084
1.3	Py–$PDEA_{122}$–D	128	128	0.190
1.4	Py–$PDEA_{150}$–D	109	109	0.121
2	C–$PDEA_{76}$–D	107	105	0.307
3	E–$PDEA_{74}$–D	104	104	0.133
4[e)]	Py–$PDEA_{100}$–Br	-	-	-
5[e)]	E–$PDEA_{82}$–Br	-	-	-
6	Py–$PNIPAM_{72}$–D	202	179	0.101
7	C–$PNIPAM_{115}$–D	86	41	0.349
8	Py–$PEEA_{78}$–D	141	134	0.013

[a)]End groups: Py: pyrene; D: dodecyl carbonotrithiocarbonate; C: Isobutyric acid, which is protonated at low pH; E: ethyl ester; [b)]*Z*-averaged diameter by DLS by intensity; [c)]*Z*-averaged diameter by DLS by number; [d)]Polydispersity of particles by DLS. [e)]Data quality is too poor to be analyzed by Cumulant method.

diffusion coefficient (D) using the Stokes–Einstein equation. According to this equation, DLS analysis revealed that the hydrodynamic diameters (D_h) of the structures prepared at 5.0 mg/mL are 255, 150, 128, and 109 nm, respectively when the degree of polymerization of DEA was increased from 23, 76 to 122 to 150 (going from polymers **1.1** to **1.4**) (Table 1). This decrease in size upon increasing hydrophilic block ratio has been observed in related ABA triblock systems.[48] The above results are perhaps related to the decrease in the relative ratio of hydrophobic end groups to hydrophilic polyelectrolyte upon increasing the polymer chain length. For comparison the weight percentage of the hydrophobic end groups in **1.1** is 10.2%, with this value decreasing to 3.32 wt% in **1.2**, to 2.09 in **1.3** and 1.71 wt% in **1.4**. In addition, the nature of the hydrophobic end group was found to affect the final morphology and particle size, cf. the difference in size observed for **1.2** versus **2** and **3**, which have very similar polymer chain lengths. The distribution of nanostructures for **2** is surprisingly high compared to the other assembly forming systems, this will be discussed in more detail in Section 2.5.

2.4. TEM Analysis

To further examine the structure of the assemblies formed from polymers **1–3**, traditional transmission electron microscopy (TEM) on graphene oxide (GO), as well as cryo-TEM were used to image the aggregates formed from these homopolymers. A spherical aggregate morphology was suggested by traditional TEM analysis of self-assemblies from polymer **1.2**, at 5.0 mg/mL on GO as a support (Figure S3, SI). On this support the sample could be viewed by traditional TEM directly on the GO grid without any staining, yet surprisingly no bilayer contrast was observed and indeed the particles looked solid, perhaps suggesting a complex internal micellar structure. To further confirm this cryo-TEM analysis of the structures was obtained and the lack of contrast clearly confirms the solid nature of the particle (**Figure 4**).

2.5. Effect of Homopolymer Concentration

ABA′ type copolymers are known to assemble into flowerlike structures, with a shell of loops of polymer B, at low concentration due to intramolecular close association.[49,50] However at higher concentrations, these intramolecular loops dissociate in favor of chains that connect two micelles and this open association can lead to aggregation and even gelation.[51,52] The PDEA homopolymers were dissolved in water at pH 2 at a range of concentrations from 0.1 to 10 mg/mL. As shown in **Figure 5**, for homopolymer **1.2** (Py–$PDEA_{76}$–D), DLS studies revealed that large relatively well-defined nanostructures >100 nm formed when the polymer concentration was higher than 1.0 mg/mL, which alongside the TEM analysis was attributed to the formation of aggregated micelles. The correlation functions of these nanostructures are well fitted by Cumulants method, and the size averaged by intensity, volume, and number are reasonably consistent (Figure S4 and Table S2, SI). Polymer nanostructures prepared at 10.0, 5.0, and 1.0 mg/mL were well-defined, and the aggregate size decreases steadily with a decrease of polymer concentration from 189 to 94 nm. Given the monomodal distributions of aggregates it does not appear that nanostructure clusters are forming as has been observed in related triblock systems.[53] A recent report by Laschewsky using RAFT to prepare a triblock with relatively short hydrophobic blocks also demonstrated similar behavior at similar concentrations, and this was attributed to the strongly hydrophobic blocks which prevented interconnected bridged micelle formation.[48] When the concentration was 0.5 mg/mL, the majority of the assemblies are proposed to be polymer micelles of ca. 30 nm (Figure 5), thus suggesting a transition from complex internal micelles to simple spherical micelles upon dilution of the sample. However, in the intensity-averaged plot (Figure S4, SI), there appears to be a mixture of

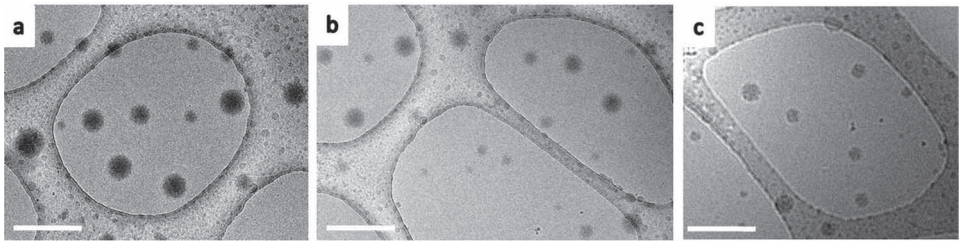

Figure 4. Representative cryo-TEM images of **1.2** (averge diameter, D_{av} = 146 nm), **2** (D_{av} = 98 nm), and **3** (D_{av} = 96 nm). Scale bar = 300 nm.

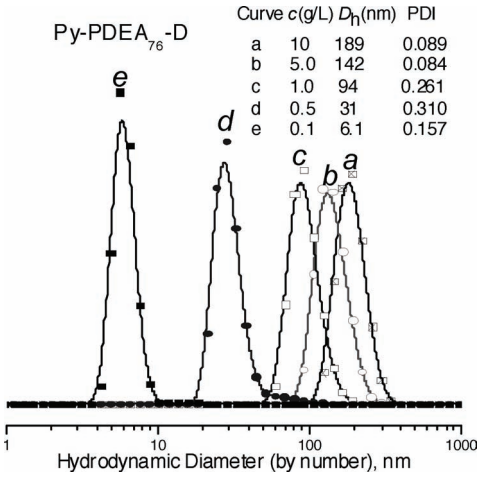

Figure 5. DLS studies of homopolymer nanostructures prepared by direct dissolution of **1.2** (Py–$PDEA_{76}$–D) in water at pH 2 at different concentrations (the corresponding correlation functions and intensity-averaged size distribution are shown in Figure S2, SI). *c* and PDI represent concentration and polymer dispersity, respectively.

structures, indicating larger structures are also present in the sample.

The micelle solution at 0.5 mg/mL of **1.2** was also examined by cryo-TEM analysis. As shown in **Figure 6**, the spherical shape is clear and the overall diameter is ~35 nm, which is consistent with the DLS results (~31 nm). Further decreasing the polymer concentration to 0.1 mg/mL affords ill-defined assemblies by DLS (intensity averaged) and indicates that this may be below or close to the critical micelle concentration (cmc) of the homopolymers. This was confirmed by determining the cmc of the homopolymers (**2** and **3**) using *N*-phenyl-1-naphthylamine (PNA) as a probe (Figure S5, SI).[54] Homopolymers **2** (C–$PDEA_{76}$–D) and **3** (E–$PDEA_{74}$–D) demonstrated similar self-assembly behavior to polymer **1.2** upon changing the polymer concentration, with a decrease in nanostructure size with decreasing concentration (Figure S6 and S7, SI). The higher cmc value compared to conventional diblock copolymer systems (ca. 1–3 mg/L) most likely results from the low hydrophobic:hydrophilic balance.[55] Furthermore, it is known that ABA block copolymers have high cmc values due to the unfavorable entropy contribution related to the bending of the hydrophilic block.[56] A summary of the DLS studies of polymers **1.2**, **2**, and **3** are shown in **Figure 7** (see also Table S2, SI). These observations can be related to the cmc of the polymers and indicates that the polymer with the most hydrophobic end α-group (**1.2**) has the lowest cmc (although this could be not confirmed using fluorescence measurements using PNA due to the interference with absorbance's from the pyrene end group), compared to polymers **2** and **3**. Indeed polymer **2** which contains the protonated carboxylic acid end group displays a rather high cmc in the region of 1 mg/mL compared to the other polymers studied in this work which were closer to 0.1 mg/mL. It should be noted that these homopolymer assemblies certainly have higher cmc values than diblock assemblies however they do offer the advantage that they can be readily assembled at relatively high concentrations.

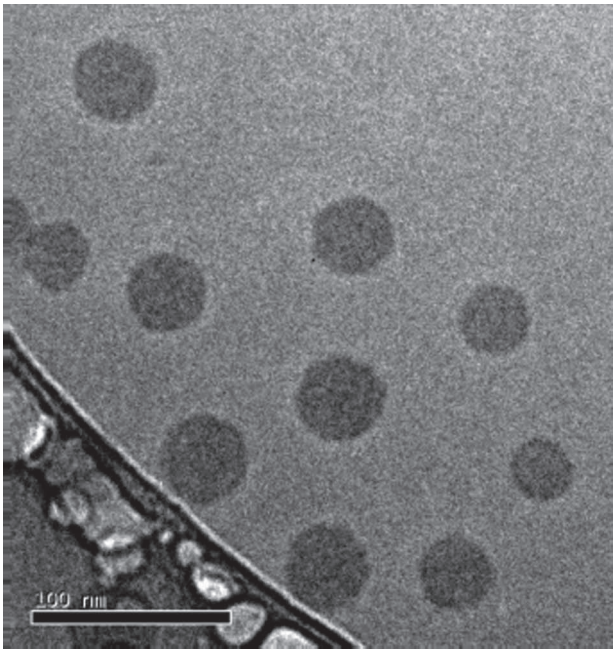

Figure 6. Representative cryo-TEM of polymer **1.2** assembled at 0.5 mg/mL and pH = 2.

2.6. Static Light Scattering (SLS) Characterization

To confirm the proposed solid morphology of these nanostructures, we utilized a combination of SLS and DLS techniques. The radius of gyration, R_g, is defined as the mass-weighted average distance from the center of mass to each mass element, which was measured by monitoring the angular dependence of the sample scattering intensity in SLS, whereas the hydrodynamic radius, R_h, is the representative of the size of a hard sphere that diffuses at the same rate as the particle being measured, which is measured by DLS. It is well known that the structure of self-assemblies can be roughly estimated by R_g/R_h ratio. For hard spheres, the theoretical value is 0.77;

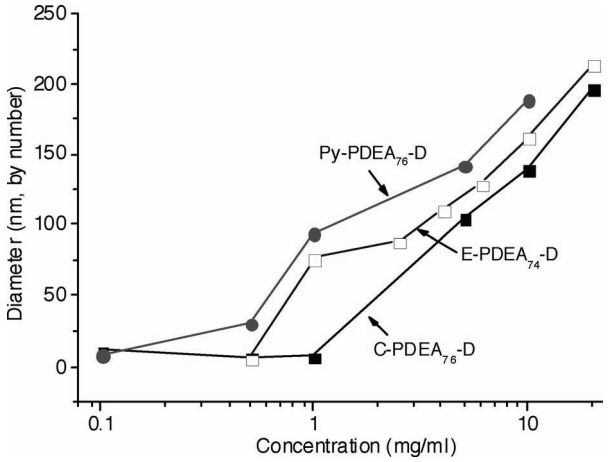

Figure 7. The particle diameter determined by DLS (by number) as a function of polymer concentration in water at pH 2 for three PDEA homopolymers: **1.2**, **2**, and **3**.

small NANO MICRO

for vesicles, the value is 1.0; for cylinders, the value is ca. 2. Hence to confirm a solid complex micelle morphology for the nanostructures formed from polymer **1.2**, we performed SLS measurements at a range of concentrations and angles. Given the concentration size dependence observed for these samples often a narrow window of concentrations was required to ensure reproducible and meaningful results. The data was analysed using a Zimm plot and the resultant R_g/R_h value was calculated to be 0.81, which is very close to the theoretical value for solid spherical particles. This was repeated for polymers **2** and **3**, and the calculated the R_g/R_h values were 0.83 and 0.80, respectively, which are close to 0.77 and thus confirmed a solid morphology (Figure S8, SI). We proposed based on the DLS, SLS, TEM, and NMR data that the homopolymer forms a complex internal micelle with an exterior structure of positively charged chains and flowerlike micelles in its interior.

2.7. Effect of The Polymer Type

The effect of the nature of the polymer chain on the self-assembly was also studied. Thermoresponsive PNIPAM homopolymers with different end groups, Py–$PNIPAM_{72}$–D (**6**) and C–$PNIPAM_{115}$–D (**7**) were synthesized by RAFT and their self-assemblies at 25 °C (Table S1, SI) and different concentrations were investigated by DLS analysis. At 25 °C the PNIPAM homopolymer is hydrophilic and can be dissolved in water directly (Figure S9, SI). Upon dissolution the *Z*-averaged diameter of particles from polymer **6** at pH≈6 was ~200 nm by DLS at 5.0 mg/mL with a PD of 0.101 (Figure S10, SI). The particles were furthered characterized by TEM, with some evidence of internal structure suggesting a solid particle structure (**Figure 8**). It has not been possible to obtain conclusive evidence as to the exact structure of these solid particles; however we propose they could be internal micellar structures such as compound micelles or more complex micellar structures similar to those recently reported independently by Pochan and Sommerdijk and their co-workers.[57–59] Polymer **7** was also dissolved in water at pH 6 at 5.0 mg/mL; however no ordered self-assembly was found at this pH, which can be attributed to the single hydrophobic end group. However upon decreasing the solution pH to 2 (and protonating the carboxylic acid group to form a second less polar end group), relatively small particles (41 nm, PD 0.349) were observed, which were considered to be polymer micelles (Figure S11, SI). This confirms that less polar dual end groups are very important for well-defined nanostructure formation. To further demonstrate the widespread effect of end group on self assembly another polymer Py–$PEEA_{78}$–D (**8**) was prepared by RAFT. This polymer is water soluble at neutral pH and was found to assemble into aggregates (D_h = 141 nm, PD = 0.013) (Figure S12 and S13, SI). With pyrene and dodecyl end groups, PDEA, PEEA, and PNIPAM homopolymers can self-assemble into well-defined nanostructures. PDEA homopolymers with carboxylic acid and dodecyl end groups, can form similar structures, at low pH, whereas PNIPAM homopolymers under the same conditions form individual micelles, rather than larger compound structures. This may in part be due to the polyelectrolyte nature of the PDEA, which due to ionic repulsion favors the formation of highly aggregated solid structures. This indicates that the polymer chains may themselves affect the morphology of the resultant nanostructure; however, it is clear that hydrophobic end groups, which are often introduced through RAFT polymerization techniques should not be ignored when considering the self assembly of hydrophilic homopolymers.

3. Conclusion

In summary, a new class of polyamine homopolymers were synthesized by RAFT and ATRP. These hydrophilic homopolymers (upon protonation) with one small hydrophobic and one less polar end group in both α and ω positions can be directly dissolved in acidic water to form well-defined aggregates, which were confirmed by ^{1}H NMR, DLS, SLS, and TEM studies. The homopolymers with a single small

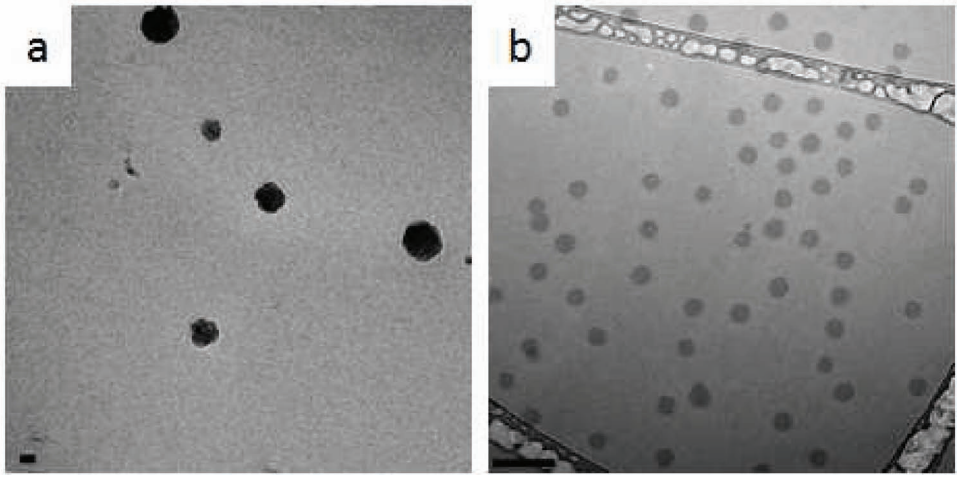

Figure 8. Representative cryo-TEM images for a) **6** (D_{av} = 197 nm) and b) **7** (D_{av} = 38 nm) assembled at 5.0 mg/mL. Scale bar = 100 nm.

hydrophobic end groups did not self-assemble into regular nanostructures in aqueous solution; however the introduction of a second less polar or hydrophobic group at the other chain end afforded well-defined aggregates. The aggregate size was observed to decrease with the decrease of the polymer concentration or the hydrophobicity of the end groups. In addition, hydrophilic (and neutral) PNIPAM and PEEA with two small hydrophobic end groups were both confirmed to form large well-defined aggregates under similar conditions. In this work we highlight that end groups introduced through RAFT polymerization, despite representing a low volume fraction of the homopolymer, significantly affect the resultant self-assembly behavior of the homopolymers. Using RAFT a wide range of functional CTAs and hydrophilic polymerizable monomers are accessible and makes the future of homopolymer self-assembly very promising. This is true especially as compared to traditional self-assembly methods, which uses di- or triblock copolymers. The preparation and characterization of homopolymers is simpler and more cost effective, hence the understanding of their self-assembly represents an important advance in the field.

4. Experimental Section

Materials: AIBN (2,2′-Azobis(2-methylpropionitrile)) was recrystallized from a 9:1 mixture of hexanes/acetone and stored in the dark at 4 °C. Diethyl aminomethacrylate (DEA) and ethoxyethyl acrylate (EEA) was purified via vacuum distillation over CaH_2 and then stored at 4 °C. NIPAM was recrystallized from a 9:1 mixture of hexanes/acetone and stored at 4 °C. Other reagents were purchased from Aldrich and used as received. DDMAT, ethyl-DDMAT and pyrene-DDMAT were synthesized as reported previously.[47,60,61] When used, dry solvents were collected and used directly from an in-house drying and degassing solvent tower delivery system. Dialysis tubing was purchased from Medicell International Ltd. with a molecular weight cut-off of 1000 Da.

Characterization: Tetrahydrofuran (THF) GPC. The molecular-weight distributions of the PDEA homopolymers were assessed at 30 °C using a Polymer Laboratories PL-GPC50 Integrated GPC system equipped with a Polymer Laboratories pump, a PLgel 5 μm MIXED-C column (300 × 7.5 mm), a WellChrom K-2301 refractive index detector, a viscometry detector, and a PD 2020 light scattering detector. The calibration was carried out using six poly(methyl methacrylate) standards with M_p values ranging from 1310 to 211 400 Da. The eluent was THF containing 2.0% (v/v) triethylamine and 0.05% (w/v) butylated hydroxytoluene, and the flow rate was 1.0 mL/min. The data were processed using Cirrus GPC offline GPC/SEC software (version 2.0).

^{1}H NMR Spectra: We recorded the spectra using a Bruker AV 400 (400 MHz) spectrometer, with long delay times, at ambient temperature using either $CDCl_3$, $CD_3OD/CDCl_3$, D_2O/H_2O or D_2O as solvents. When D_2O/H_2O was used as solvent, the ^{1}H NMR experiment with water suppression option was selected.

TEM: TEM images were obtained using a JEOL electron microscope operating at 200 kV equipped with a LaB6 gun and a Gatan digital camera. To prepare TEM samples, 2 μL of an aqueous nanostructure solution was placed on a graphene oxide (GO) grid for 60 s, and the water droplet was blotted away and then left to air dry.

Cryo-TEM: Sample preparation was carried out using a Cryo-Plunge 3 unit (Gatan Instruments) employing a double blot technique. 3 μL of sample (with negative stain, 0.45% uranium acetate, 0.9% trehalose, and 68% of original sample concentration, for Figure 4) was pipetted onto a plasma etched (15 s) 400 mesh holey carbon grid (Agar Scientific) held in the plunge chamber at approx 90% humidity. The samples were blotted, from both sides for 0.5, 0.8, or 1.0 s, depending on sample viscosity. The samples were then plunged into liquid ethane at a temperature of −170 °C. The grids were blotted to remove excess ethane then transferred, under liquid nitrogen to the cryo-TEM specimen holder (Gatan 626 cryo holder) at −170 °C. Samples were examined using a Jeol 2100 TEM operated at 200KV and imaged using a Gatan Ultrascan 4000 camera and images captured using Digital Micrograph software (Gatan).

DLS: DLS studies of aqueous nanostructures were conducted over a range of solution pH at a fixed scattering angle of 173°. The data were processed by Cumulants analysis of the experimental correlation function, and aggregate diameters were calculated from the computed diffusion coefficients using the Stokes–Einstein equation. Each reported measurement was the average of three runs.

SLS: SLS analysis was performed on a Malvern Instruments Autosizer 4800 equipped with an APD detector and a Malvern 7132 50 ns 16-bit digital auto-correlator, using a 50 mW green incident laser beam. SLS data was collected for 4 or more different concentrations of the aggregates, 20 different angles for each concentration. The data were analyzed using the Zimm plot method on Malvern PSW0078 Advanced software to determine R_g.

Synthesis of Pyrene-Based ATRP Initiator: A flask with a magnetic flea was charged with 1-pyrenemethanol (1.000 g; 4.219 mmol), anhydrous THF (30 mL), TEA (0.4744 g; 4.641 mmol). This flask was placed in an ice bath. 2-Bromoisobutyryl bromide (1.089 g; 4.641 mmol) was then added dropwise. Precipitation was immediately observed. After 5 h, 1 mL of methanol was added and reacted for 20 min. THF and residual methanol was removed by rotator evaporator. The yellow crude product is solid, with a black and viscous fluid as byproduct. The product was then extracted with 100 mL of 0.01 M NaOH water for 1 h, then washed with neutral water 3 times. The crude product was then recrystallized in methanol twice to give a yellow product. Yield: 37%. ^{1}H NMR spectrum: 8.35–8.0 (m, pyrene, 9H); 5.93 (s, Py–CH_2–O, 2H); 1.94 [s, OOC–$C(CH_3)_2$Br, 6H].

RAFT Synthesis of PDEA Homopolymer: In a typical RAFT protocol, a flask with a magnetic flea and a rubber septum was charged with AIBN radical initiator (3.0 mg; 1.8×10^{-2} mmol), pyrene–DDMAT CTA (94.0 mg; 0.162 mmol), DEA monomer (3.039 g; 16.2 mmol), and dioxane (8.12 mL). This solution was deoxygenated using a N_2 sparge for 30 min before heating at 80 °C under a nitrogen atmosphere. The [DEA]:[pyrene-DDMAT]:[AIBN] relative molar ratios were 100:1:0.2. After 4.5 h, the monomer conversion was 76% as judged by ^{1}H NMR. The final reaction solution was diluted with acetone and 0.01 M HCl aqueous solution and then purified by dialysis against water at pH 2–4. A fine white powder was obtained after freeze-drying. A ^{1}H NMR spectrum of the purified block copolymer was recorded using a D_2O as solvent.

ATRP Synthesis of PDEA Homopolymer: In a typical ATRP protocol, a flask with a magnetic flea and a rubber septum was charged with ethyl 2-bromoisobutyrate initiator (50.0 mg;

small NANO MICRO

0.260 mmol), bipyridine (bpy) ligand (80.1 mg; 0.52 mmol), DEA monomer (4.077 g; 21.8 mmol), and methanol (10 mL). This solution was deoxygenated using a N_2 sparge for 30 min before adding Cu(I)Br (36.8 mg, 0.26 mmol). The [DEA]:[2-bromoisobutyrate]:[CuBr]:[bpy] relative molar ratios were 85:1:1:2. The DEA polymerization was conducted under a nitrogen atmosphere at 20 °C. After 2.5 and 20 h, the monomer conversions were 50% and 96.5%, respectively, as judged by ^{1}H NMR. The final reaction solution was diluted with acetone and 0.01 M HCl aqueous solution and purified by dialysis against water at pH 2–4. A fine off-white powder was obtained after freeze-drying. A ^{1}H NMR spectrum of the purified block copolymer was recorded using a D_2O as solvent.

RAFT Synthesis of PNIPAM or PEEA Homopolymers: In a typical RAFT protocol, a flask with a magnetic flea and a rubber septum was charged with AIBN radical initiator (2.0 mg; 1.2×10^{-2} mmol), pyrene-DDMAT CTA (42.0 mg; 7.2×10^{-2} mmol), monomer (5.77 mmol) and dioxane/dimethylformamide (DMF) (2.8 mL each). This solution was deoxygenated using a N_2 sparge for 60 min before heating at 65 °C under a nitrogen atmosphere. The [NIPAM]:[pyrere-DDMAT]:[AIBN] relative molar ratios were 100:1:0.3. After 5.5 h, the monomer conversion is 75%, and after 24 h, the conversion is 95% as judged by ^{1}H NMR. The precipitation by diethyl ether in the presence of dry ice only yields 10% of product. Thus water was added into the polymer solution in DMF and then dialyzed against water. The fine powder was obtained by freeze drying in a yield of 78%. ^{1}H NMR spectrum of the purified homopolymer was recorded using dimethylsulfoxide (DMSO)-d_6 or D_2O as solvent to investigate the self-assembly.

Preparation of Aggregates: Typically PDEA homopolymer (100.0 mg, varying at different copolymer concentrations) was dissolved into 10.00 g pure water at pH 2 at room temperature to form nanostructures directly. PNIPAM homopolymers were dissolved in neutral water and stirred for 2 h.

Supporting Information

Supporting Information is available from the Wiley Online Library or from the author.

Acknowledgements

The EPSRC, Leverhulme Trust and Royal Society are thanked for funding. The GPC used in this research was obtained through Birmingham Science City: Innovative Uses for Advanced Materials in the Modern World (West Midlands Centre for Advanced Materials Project 2), with support from Advantage West Midlands (AWM) and partly funded by the European Regional Development Fund (ERDF). We thank (Wellcome Trust grant reference: 055663/Z/98/Z) for the cryo-instrument use in the electron microscopy facility at Warwick. We also thank Drs. Steve Furzeland and Derek Atkins from Unilever for assistance with the cryo-TEM.

This Full Paper is part of the Special Issue dedicated to Chad Mirkin in celebration of 20 years of influential research at Northwestern University.

[1] M. Antonietti, S. Förster, *Adv. Mater.* **2003**, *15*, 1323.
[2] J. Du, R. K. O'Reilly, *Soft Matter* **2009**, *5*, 3544.
[3] R. K. O'Reilly, C. J. Hawker, K. L. Wooley, *Chem. Soc. Rev.* **2006**, *35*, 1068.
[4] E. S. Read, S. P. Armes, *Chem. Commun.* **2007**, 3021.
[5] S. Holder, N. A. J. M. Sommerdijk, *Polym. Chem.* **2011**, *2*, DOI: 10.1039/c0py00379d.
[6] J. Rodriguez-Hernandez, F. Checot, Y. Gnanou, S. Lecommandoux, *Prog. Polym. Sci.* **2005**, *30*, 691.
[7] H. Cui, Z. Chen, S. Zhong, K. L. Wooley, D. J. Pochan, *Science* **2007**, *317*, 647.
[8] R. C. Hayward, D. J. Pochan, *Macromolecules* **2010**, *43*, 3577.
[9] J. Isrealachvili, *J. Chem. Soc., Faraday Trans.* **1976**, *72*, 1525.
[10] D. E. Discher, A. Eisenberg, *Science* **2002**, *297*, 967.
[11] C. Tanford, *Science* **1978**, *200*, 1012.
[12] L. Zhang, A. Eisenberg, *J. Am. Chem. Soc.* **1996**, *118*, 3168.
[13] J. N. Cha, H. Birkedal, L. E. Euliss, M. H. Bartl, M. S. Wong, T. J. Deming, G. D. Stucky, *J. Am. Chem. Soc.* **2003**, *125*, 8285.
[14] S. Basu, D. R. Vutukuri, S. Thayumanavan, *J. Am. Chem. Soc.* **2004**, *127*, 16794.
[15] T. S. Kale, A. Klaikherd, B. Popere, S. Thayumanavan, *Langmuir* **2009**, *25*, 9660.
[16] S. Arumugam, D. R. Vutukuri, S. Thayumanavan, V. Ramamurthy, *J. Am. Chem. Soc.* **2005**, *127*, 13200.
[17] Z. Hordyjewicz-Baran, L. You, B. Smarsly, R. Sigel, H. Schlaad, *Macromolecules* **2007**, *40*, 3901.
[18] X. Yu, S. Zhong, X. Li, Y. Tu, S. Yang, R. M. Van Horn, C. Ni, D. J. Pochan, R. P. Quirk, C. Wesdemiotis, W. B. Zhang, S. Z. D. Cheng, *J. Am. Chem. Soc.* **2010**, *132*, 16741.
[19] T. Gadt, N. S. Ieong, G. Cambridge, M. A. Winnik, I. Manners, *Nat. Mater.* **2009**, *8*, 144.
[20] N. Petzetakis, A. P. Dove, R. K. O'Reilly, *Chem. Sci.* **2011**, *2*, 955.
[21] M. Lazzari, M. A. Quitela, *Macromol. Rapid Commun.* **2009**, *30*, 1785.
[22] F. Grohn, K. Klein, K. Koynov, *Macromol. Rapid Commun.* **2010**, *31*, 75.
[23] Z. Li, E. Kesselman, Y. Talmon, M. A. Hillmyer, T. P. Lodge, *Science* **2004**, *306*, 98.
[24] S. H. Kim, J. P. K. Tam, F. Nederberg, K. Fukushima, Y. Y. Yang, R. M. Waymouth, J. Hedrick, *Macromolecules* **2009**, *42*, 25.
[25] S. Furyk, Y. Zhang, D. Ortiz-Acosta, P. S. Cremer, D. E. Bergbreiter, *J. Polym. Sci. Part A: Polym. Chem.* **2006**, *44*, 1492.
[26] M. Changez, N. G. Kang, C. H. Lee, J. S. Lee, *Small* **2010**, *6*, 63.
[27] F. Lo Verso, C. N. Likos, *Polymer* **2008**, *49*, 1425.
[28] M. Rubinstein, A. V. Dobrynin, *TRIP* **1997**, *5*, 181.
[29] A. N. Semonov, J. F. Joanny, A. R. Khokhlov, *Macromolecules* **1995**, *28*, 1066.
[30] A. N. Semonov, I. A. Nyrkova, A. R. Khokhlov, *Macromolecules* **1995**, *28*, 7491.
[31] A. N. Semonov, M. Rubinstein, *Macromolecules* **1998**, *31*, 1373.
[32] J. P. Kaczmarski, J. E. Glass, *Macromolecules* **1993**, *26*, 5149.
[33] O. Vorobyova, A. Yekta, M. A. Winnik, W. Lau, *Macromolecules* **1998**, *31*, 8998.
[34] Y. Wang, M. A. Winnik, *Langmuir* **1990**, *6*, 1437.
[35] D. W. Smithenry, M. S. Kang, V. K. Gupta, *Macromolecules* **2001**, *34*, 8503.
[36] J. Chiefari, Y. K. Chong, F. Ercole, J. Krstina, J. Jeffery, T. P. T. Le, R. T. A. Mayadunne, G. F. Meijs, C. L. Moad, G. Moad, E. Rizzardo, S. H. Thang, *Macromolecules* **1998**, *31*, 5559.
[37] G. Moad, E. Rizzardo, S. H. Thang, *Aust. J. Chem.* **2005**, *58*, 379.
[38] S. Perrier, P. Takolpuckdee, *J. Polym. Sci. Part A: Polym. Chem.* **2005**, *43*, 5347.
[39] G. Moad, Y. K. Chong, A. Postma, E. Rizzardo, S. H. Thang, *Polymer* **2005**, *46*, 8458.

[40] H. Willcock, R. K. O'Reilly, *Polym. Chem.* **2010**, *1*, 149.
[41] A. O. Moughton, R. K. O'Reilly, *Chem. Commun.* **2010**, *46*, 1091
[42] P. Kujawa, H. Watanabe, F. Tanaka, F. M. Winnik, *Eur. Phys. J. E* **2005**, *17*, 129.
[43] T. Koga, F. Tanaka, R. Motokawa, S. Koizumi, F. M. Winnik, *Macromolecules* **2008**, *41*, 9413.
[44] J. Xu, L. Tao, C. Boyer, A. B. Lowe, T. P. Davies, *Macromolecules* **2011**, *44*, 299.
[45] W. Kong, B. Li, Q. Jin, D. Ding, *Langmuir* **2010**, *26*, 426.
[46] Y. Han, H. Yu, H. Du, W. Jiang, *J. Am. Chem. Soc.* **2010**, *132*, 1144.
[47] J. Du, R. K. O'Reilly, *Macromol. Chem. Phys.* **2010**, *211*, 1530.
[48] A. M. Bivigou-Koumba, E. Gornitz, A. Laschewsky, P. Muller-Buschbaum, C. M. Papadakis, *Colloid Polym. Sci.* **2010**, *288*, 499.
[49] T. Annable, R. Buscall, R. Ettelaie, D. Whittlestone, *J. Rheol.* **1993**, *37*, 695.
[50] A. Yekta, J. Duhamel, H. Adiwidjaja, P. Brochard, M. A. Winnik, *Langmuir* **1993**, *9*, 881.
[51] V. Castelletto, I. M. Hamley, Y. Ma, X. Bories-Azeau, S. P. Armes, A. L. Lewis, *Langmuir* **2004**, *20*, 4306.
[52] K. Van Butsele, S. Cajot, S. Van Vlierberghe, P. Dubruel, C. Passirani, J. P. Benoit, R. Jerome, C. Jerome, *Adv. Funct. Mater.* **2009**, *19*, 1416.
[53] C. Booth, D. Attwood, *Macromol. Rapid Commun.* **2000**, *21*, 501.
[54] P. Xu, H. Tang, S. Li, J. Ren, E. Van Kirk, W. J. Murdoch, M. Radosz, Y. Shen, *Biomacromolecules* **2004**, *5*, 1736.
[55] M. Wilhelm, C. L. Zhao, Y. Wang, R. Xu, M. A. Winnik, *Macromolecules* **1991**, *24*, 1033.
[56] T. Liu, K. Kim, B. S. Hsiao, B. Chu, *Polymer* **2004**, *45*, 7989.
[57] K. Hales, Z. Y. Chen, K. L. Wooley, D. J. Pochan, *Nano Lett.* **2008**, *8*, 2023.
[58] B. E. McKenzie, F. Nudelman, P. H. H. Bomans, S. J. Holder, N. Sommerdijk, *J. Am. Chem. Soc.* **2010**, *132*, 10256.
[59] A. L. Parry, P. H. H. Bomans, S. J. Holder, N. Sommerdijk, *Angew. Chem. Int. Ed.* **2008**, *47*, 8859.
[60] J. Skey, R. K. O'Reilly, *Chem. Commun.* **2008**, 4183.
[61] A. C. Evans, A. Lu, C. Ondeck, D. A. Longbottom, R. K. O'Reilly, *Macromolecules* **2010**, *43*, 6374.

Received: February 25, 2011
Revised: April 20, 2011
Published online: June 7, 2011